Neuropsychologia 65 (2014) 197–210

Contents lists available at ScienceDirect

Neuropsychologia

journal homepage: www.elsevier.com/locate/neuropsychologia

Similarities between explicit and implicit motor imagery in mental rotation of hands: An EEG study

Bethel. A. Osuagwu *, Aleksandra Vuckovic

Centre for Rehabilitation Engineering, University of Glasgow, University Avenue, Glasgow G12 8QQ, UK

ARTICLE INFO

Article history:
Received 4 June 2014
Received in revised form
16 September 2014
Accepted 21 October 2014
Available online 30 October 2014

Keywords:
Mental rotation
Motor imagery
Sensorimotor cortex
EEG
Source localisation
sLORETA

ABSTRACT

Chronometric and imaging studies have shown that motor imagery is used implicitly during mental rotation tasks in which subjects for example judge the laterality of human hand pictures at various orientations. Since explicit motor imagery is known to activate the sensorimotor areas of the cortex, mental rotation is expected to do similar if it involves a form of motor imagery. So far, functional magnetic resonance imaging and positron emission tomography have been used to study mental rotation and less attention has been paid to electroencephalogram (EEG) which offers a high time-frequency resolution. The time-frequency analysis is an established method for studying explicit motor imagery. Although hand mental rotation is claimed to involve motor imagery, the time-frequency characteristics of mental rotation have never been compared with those of explicit motor imagery. In this study, time-frequency responses of EEG recorded during explicit motor imagery and during a mental rotation task, inducing implicit motor imagery, were compared. Fifteen right-handed healthy volunteers performed motor imagery of hands in one condition and hand laterality judgement tasks in another while EEG of the whole head was recorded. The hand laterality judgement was the mental rotation task used to induce implicit motor imagery. The time-frequency analysis and sLORETA localisation of the EEG showed that the activities in the sensorimotor areas had similar spatial and time-frequency characteristics in explicit motor imagery and implicit motor imagery conditions. Furthermore this sensorimotor activity was different for the left and for the right hand in both explicit and implicit motor imagery. This result supports that motor imagery is used during mental rotation and that it can be detected and studied with EEG technology. This result should encourage the use of mental rotation of body parts in rehabilitation programmes in a similar manner as motor imagery.

1. Introduction

When attempting to judge the laterality of a picture of a human hand, it is believed that subjects mentally rotate an internal representation of their own hand in order to match it with the presented hand (Cooper & Shepard, 1975). Such a task is referred to as hand laterality test/judgement task (HLT) (Moseley, Butler, Beames, & Giles, 2012). A degree of mental effort applied in this task is proportional to the degree of mental rotation.

This rotation is similar to the mental rotation used for searching the congruency between two 3-D objects (Shepard & Metzler, 1971), in which subjects holistically, mentally rotate one of the 3D objects to match its orientation with that of the other (Cooper & Shepard, 1975). This holistic mental rotation model is supported by neuroimaging studies of mental rotation consistently finding the activation of the superior parietal lobule (SPL) and the intraparietal sulcus (BA 40). These are brain areas known for implementation of spatial maps that code the position of body parts in relation to each other (Zacks, 2008; Sakata, Takaoka, Kawarasaki, & Shibutani, 1973; Bonda, Petrides, Frey, & Evans, 1995). Remarkably, activities in these regions are proportional to the degree of mental rotation performed (Gogos et al., 2010; Zacks, 2008; Weiss et al., 2009).

The hand mental rotation does not violate the bio-mechanical constraints imposed by the joints (Parsons, 1987a, 1987b, 1994). As shown by several chronometric studies, the time (reaction time, RT) it takes to mentally rotate the hand is proportional to the angular disparity between the current hand orientation and the new orientation (Shepard & Metzler, 1971; Parsons et al., 1995). Most interestingly, this time is also proportional to the time it would take to perform the movement physically (Parsons, 1994). These findings suggest that the neural system of movement is used to mentally rotate the hand in order to make a match with the presented hand picture. Since there is no overt movement, the neural system should resemble that of Motor Imagination/Imagery (MI) which is the mental simulation of motor action (Lotze & Halsband, 2006; Jeannerod, 2006). MI is neurally similar to physical execution of the action except that no movement

* Corresponding author.
E-mail address: b.osuagwu.1@research.gla.ac.uk (Bethel.A. Osuagwu).

http://dx.doi.org/10.1016/j.neuropsychologia.2014.10.029
0028-3932/

is observed. During the mental rotation tasks, subjects are often unaware of imagination of movement. For this reason the term 'implicit MI' is used to describe the unrequested/unconscious imagination of movement during mental rotation tasks (Parsons, 2001; Parsons et al., 1995). Explicit MI therefore refers to a conscious motor imagination.

Implicit MI in mental rotation of body parts is an idea supported by many studies (Vingerhoets, de Lange, Vandemaele, Deblaere, & Achten, 2002; Cooper & Shepard, 1975; Parsons, 1987a, 1987b, 1994; Parsons et al., 1995; Wexler, Kosslyn, & Berthoz, 1998). Several brain areas known to be active during explicit MI have been found active during the mental rotation tasks (Zacks, 2008; Vingerhoets et al., 2002; Parsons et al., 1995). Parsons and colleagues used mental rotation induced by HLT to show that apart from the primary sensorimotor cortices, all the brain regions known to participate in the planning and execution of movement were activated by mental rotation of hands (Parsons et al., 1995).

So far extensive neuroimaging studies of mental rotation have been done using PET and fMRI which offer a high spatial resolution. EEG is a technology offering a higher temporal and frequency resolution which is useful in studying the dynamic brain processes. Time-frequency analysis of EEG is a well-established technique used to study MI (Pfurtscheller, Scherer, Müller-Putz, & Lopes da Silva, 2008). Although hand mental rotation is claimed to involve MI, the time-frequency characteristics of mental rotation have never been compared with those of MI. Such an analysis is necessary to establish the relationship between MI and hand mental rotation. Previous 3D objects and alphanumeric based mental rotation studies (Riečansky` & Katina, 2010; Gill, O'Boyle, & Hathaway, 1998) using EEG did not describe the complete time-frequency characteristics.

In a recent study, Chen and colleague (Chen, Bin, Daly, & Gao, 2013) only analysed an early induced EEG activity during hand mental rotation induced by HLT. Their experimental design involved subjects pressing buttons with their hands to indicate their judgements. Since the subjects were believed to be mentally rotating their hands, pressing the button with the same hands could interfere with the results. An important, yet unanswered question that would further confirm similarity between explicit and implicit MI is whether it is possible to discriminate between left and right mental rotation using EEG signal recorded during a hand mental rotation task such as HLT.

The present study has three main objectives. (1) To study the time-frequency dynamics and spatial localisation of sensorimotor activities during mental rotation of hands induced by HLT. (2) To test whether it is possible to discriminate between left and right hand mental rotation using EEG recorded during HLT. (3) To compare time-frequency responses over the sensorimotor cortices between implicit MI (in HLT) and explicit MI. The knowledge gained by studying the above is relevant to understanding the mental rotation process. Furthermore establishing that implicit MI is involved in mental rotation and that it is similar to explicit MI can open new areas of application in which mental rotation induced implicit MI can be used to complement explicit MI used in rehabilitation of movement (Cramer, Orr, Cohen, & Lacourse, 2007; Dijkerman, Ietswaart, Johnston, & MacWalter, 2004; Driskell, Copper, & Moran, 1994; Grangeon, Revol, Guillot, Rode, & Collet, 2012). Patients who find it difficult to perform explicit MI due to loss of proprioception/sensation for example following incomplete spinal cord injury may use the implicit MI automatically invoked in the brain to activate the motor cortex in a similar manner as explicit MI in rehabilitation. Hand mental rotation induced with HLT is already in use in the treatment of complex regional pain (Moseley et al., 2012; Walz et al., 2013; Bowering et al., 2013) and its use is expected to widen (Moseley et al., 2012).

2. Methods

2.1. Data collection

2.1.1. Subjects

Fifteen right handed (Edinburgh handedness inventory (Oldfield, 1971) mean, $+76 \pm 19$) healthy subjects (mean age 24.9 ± 5.0, 6 females) volunteered for this study. The subjects gave their informed consents. The study was approved by the University ethics committee.

2.1.2. MI trials

A cue-based paradigm implemented with rtsBCI Scherer was used. A trial lasted for 6000 ms. At the beginning of a trial ($t = -3000$ ms), the user was presented with a blank screen.

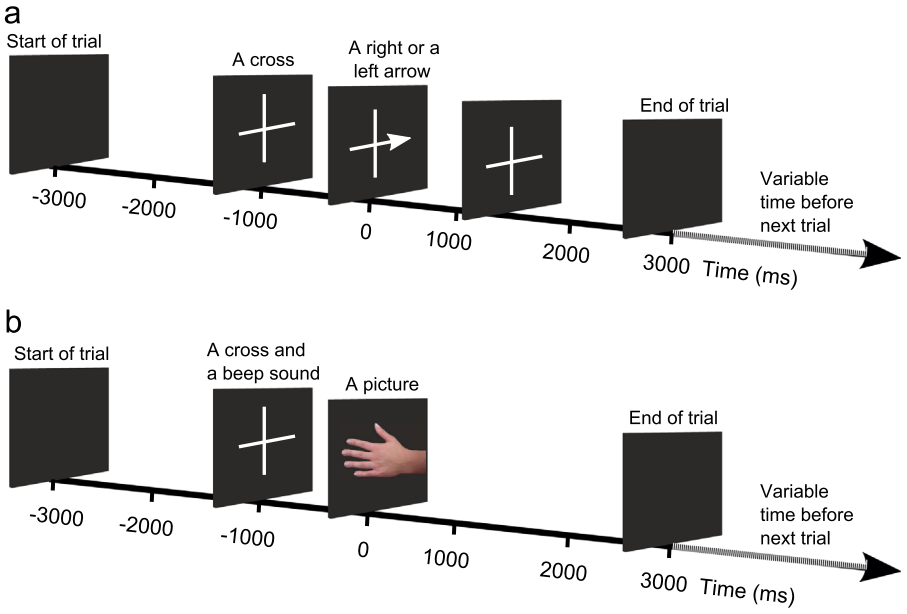

Fig. 1. The sequence of events for (a) MI and (b) HLT trials.

A warning cue (a cross) appeared on the screen at $t=-1000$ ms informing the user to get ready. This cross disappeared at the end of the trial ($t=3000$ ms). From $t=-3000$ ms to $t=0$ ms, the subjects were asked to relax, rest and they were not performing any study related task. At $t=0$ ms an execution cue (which is an arrow pointing to either left or right) was presented on the screen and stayed there till $t=1250$ ms. Depending on the cue the subjects had to perform continuous kinesthetic MI of opening and closing of the left or the right hand. This gave two types of MI condition namely, right hand MI and left hand MI. Subjects were asked to continuously imagine waving their hand from $t=0$ s till $t=3000$ ms. They were allowed to rest from $t=3000$ ms for a variable length of time (between 1000 to 3000 ms) before another trial started. This paradigm, often used in brain computer interface experiments (Vuckovic & Osuagwu, 2013), is shown in Fig. 1a.

2.1.3. HLT trials

The timing of the HLT paradigm was similar to that of MI. At $t=-1000$ ms the warning cue appeared accompanied with a beep sound. The beep sound was used as a reference for determining the subjects' response time on an audio recording explained later. At $t=0$ ms, an execution cue in the form of a hand picture was presented on the screen replacing the cross. The picture disappeared at $t=3000$ ms regardless of the subject's response. This paradigm is shown in Fig. 1b. The subjects were asked to verbally express their laterality judgement of the presented hand picture by answering 'left' or 'right'. Using verbal expression avoids hand movement unlike in the case of pushing a button to give an answer. Such a hand movement might interfere with the outcome of the experiment (Takeda, Shimoda, Sato, Ogano, & Kato, 2010). The hand pictures had plain backgrounds and each contained only one hand performing a gesture. They were processed to the size of 408 by 408 pixels. For each hand gesture there was a left and a right hand picture. Each of the pictures was presented in two orientations, counter-clockwise by 90° (CCW) and clockwise by 90° (CW). This gave four types of HLT condition namely right CCW HLT, left CW HLT, right CW HLT and left CCW HLT. The first two are termed medial orientations because they involve rotations towards the midline of the body while the last two are termed lateral orientations because they involve rotation outside the midline of the body (Parsons, 1987b). Examples of the stimuli are shown in Fig. 2.

2.1.4. Procedure

Subjects sat in an armchair facing a computer screen. Their hands were pronated and placed on a table in front of them. Subjects were instructed to relax and avoid physical movements during the experiment. They were monitored throughout the experimental session to make sure that they followed the instructions and a part of the experiment was restarted if instructions were not followed. The MI trials (which took on average only 20 min in total) were followed by HLT trials after the subjects have had about 15 min of rest. It was necessary to separate the MI runs from the HLT runs to avoid possible interference of the techniques the subjects employed (Wraga, Thompson, Alpert, & Kosslyn, 2003). For example the hand pictures might encourage visual MI during the MI trials if the MI trials were shown interchangeably with HLT trials or if the HLT runs were performed first. Also the performance of explicit motor imagery in the MI trials might influence the technique used during the HLT trials if the two conditions were presented interchangeably (Wraga et al., 2003). A total of 120 trials for MI were obtained (60 trials for each of left and right hand) divided into 4 runs of 30 trials (15 for each hand presented in a random order). A total of 240 trials for HLT were obtained (60 trials for each of right CCW, left CW, right CW and left CCW). This was divided into 6 runs of 40 trials consisting of 10 trials for each of the orientation presented in a random order. The subjects were allowed to rest between the runs. A relatively small number of trials were purposely chosen to reduce the influence of fatigue in both MI and HLT runs.

2.1.5. Data recording

Signal recording was performed under MATLAB and Simulink (MATLAB R2012a, The MathWorks Inc., Natick, MA). Electrodes were placed on 47 different locations on the scalp following the International 10/10 electrode positioning standard as shown in Fig. 3. Linked ear reference was used and the ground electrode was placed on location Afz. An electrode was attached to the lateral canthus on the orbicularis oculi of the right eye to record Electrooculogram (EOG) for the purpose of artefact detection. EEG and EOG were recorded at the sample frequency of 256 Hz using three modules of the g.USBAmp (biosignal amplifier, g.tec Medical Engineering GmbH, Austria). The impedance of the electrodes was kept below 5 kΩ. Signal was filtered online between 0.5 and 60 Hz with a notch filter at 50 Hz using the IIR digital Butterworth filters built into the amplifiers.

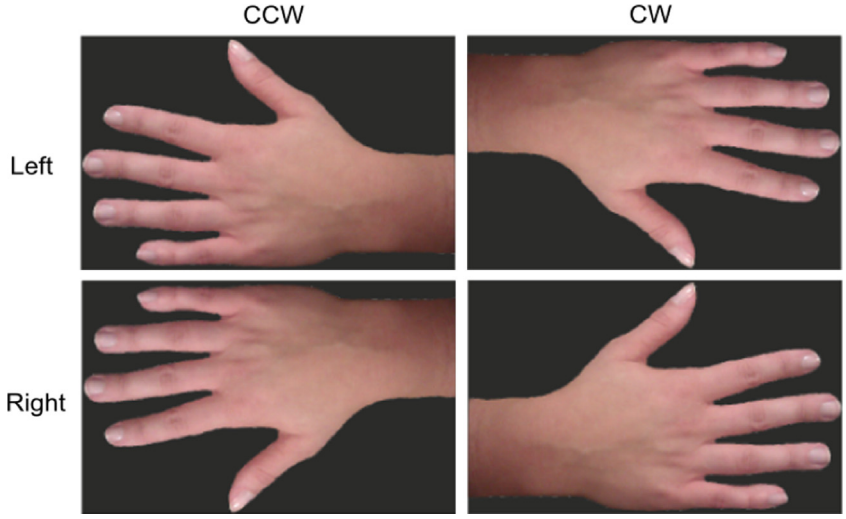

Fig. 2. The columns show the left and right stimuli while the rows show their orientations. In each column the images are mirrors of each other. The first column shows the images rotated counter-clockwise (CCW) by 90° while the second column shows images rotated clockwise (CW) by 90°. All rotations are relative to the hands at upright position.

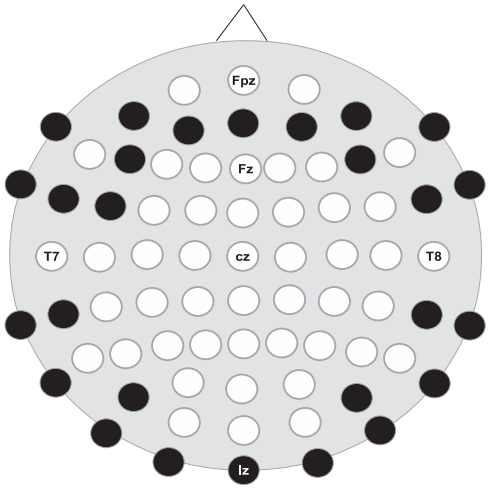

Fig. 3. The 10/10 international electrode positioning standard used for HLT and MI experiment. The black circles show unused positions.

In addition to EEG and EOG, audio signal was recorded during the HLT trials which enabled a subject to give his/her judgement by verbal response (Ionta, Fourkas, Fiorio, & Aglioti, 2007).

2.2. Data analysis

2.2.1. Behavioural data

The beep sound during the HLT trials was used to retrieve the subjects' RTs from the audio recordings. The RTs for HLT trials were obtained by splitting the recoded audio signal into trials using the beep events. The beep time point (btp) was determined at two standard deviations from the start of the beep sound wave while the subjects' response time point (rtp) was detected at five standard deviations into the subjects' response speech wave. Given that the beep occurred at $t=-1000$ ms and the stimuli appeared at $t=0$ ms into the trials, $RT=(rtp-btp)-1000$ was calculated in milliseconds. The subjects' mean RTs for the correct laterality judgements were submitted to a two-way analysis of variance (ANOVA), with hand pictures (left and right hands) and picture orientations (CW, CCW) as within subjects factors. The error rate was taken as the percentage number of trials with incorrect laterality judgement while the accuracy was calculated as 100 minus the error rate. The error rate was obtained by listening back to the audio trials for the subjects' response for each hand picture.The Wilcoxon rank sum test was used to compare the medians of the accuracies between the hands and orientations. Statistical significance level was to $p=0.05$.

2.2.2. EEG data pre-processing

The continuous EEG data of MI and HLT were split into trials. HLT trials with incorrect response were eliminated. All data were visually inspected and epochs with artefact like a sudden burst in amplitude over all electrodes were eliminated. For each subject, the MI and HLT trials were concatenated to form a single data set. The data sets were individually decomposed into 48 maximally independent temporal components using the logistic infomax independent component analysis (ICA) algorithm (Hyvärinen & Oja, 2000; Comon, 1994) implemented in EEGLAB (Delorme & Makeig, 2004). The components were visually inspected and components corresponding to ocular artefact were removed (Hoffmann & Falkenstein, 2008). All other artefacts like electrocardiogram and electromyogram (which mostly occurred when subjects gave their answers) were identified and removed by considering their typical morphology, spectrum, topography and temporal characteristics (Iriarte et al., 2003). The remaining components were back projected to EEG channels and then used for group analysis in EEGLAB and sLORETA after separating the data set back to HLT and MI trials and computing common average reference of the EEG channels.

2.2.3. Time-frequency analysis in EEGLAB

Group analysis was performed under EEGLAB to visualise and compare the Event Related Desynchronisation (ERD) (Pfurtscheller & Aranibar, 1977; Pfurtscheller & Berghold, 1989) and Event Related Synchronisation (ERS) (Pfurtscheller, 1992; Pfurtscheller & Lopes da Silva, 1999) arising from MI and HLT trials. Here ERD and ERS refer to decrease and increase respectively of EEG power relative to a baseline period within a narrow frequency band. Movement related cortical processes like those during MI and physical execution can be quantified with ERD across the sensorimotor cortex. ERD/ERS, sometimes referred to as event related spectral perturbation (Makeig, 1993), will be used in this text as a general term to refer to both ERD and ERS when necessary. ERD/ERS was computed using EEGLAB routines. The Morlet Wavelet transform was used to perform time frequency analysis of the EEG data in the frequency band 3 to 60 Hz with a Hanning-tapered window applied and the number of cycles set to 3. These wavelet parameters allowed low frequencies starting from 3 Hz to be analysed in a one second window (Young, 1993). The ERD/ERS was computed as power changes in decibels relative to a baseline period ($t=-2000$ to -1000 ms). The full description of ERD/ERS method is given in the EEGLAB's methods by Delorme and Makeig (Delorme & Makeig, 2004). ERD/ERS averaged over trials and subjects per experimental condition type is presented. Also presented are ERD/ERS scalp maps in small time windows of 200 ms and in chosen frequency bands. The statistical non-parametric method with Holm's correction for multiple comparison (Holm, 1979) was used to assess the differences in ERD/ERS within and between the conditions at $p=0.05$.

2.2.4. sLORETA localisation

Localisation of the cortical three-dimensional distribution of current density of EEG was done using the Standardised Low Resolution Electromagnetic Tomography (sLORETA) (Pascual-Marqui, 2002). The method is a linear minimum norm inverse solution to EEG 3D localisation inverse problem. The sLORETA method has been shown to have no localisation bias (Pascual-Marqui, 2007). The sLORETA (estimated current density) cortical map/image is computed for 6239 voxel partitions of intracerebral volume at 5 mm spatial resolution. Brodmann areas are reported using the Montreal Neurological Institute (MNI) space with correction to the Talairach space (Talairach & Tournoux, 1988; Brett, Johnsrude, & Owen, 2002).

The trials were split into one second long time windows. Frequency domain sLORETA was computed for each window in the frequency bands including 1–3 Hz (δ), 4–7 Hz (θ), 8–12 Hz (α/μ), 12–16 Hz ($\beta1$), 16–24 Hz ($\beta2$). Baseline was taken from the period before the warning sign ($t=-2000$ to -1000 ms). Images of sLORETA were computed over one second time windows beginning at $t=500$ ms post execution cue. Shifting the analysis window in 100 ms time steps over the period of interest and computing sLORETA image at each step yielded a temporal activation pattern of different cortical structures. The extent of activation at each time step was quantified for each brain structure by summing up the number of voxels active for that structure in the corresponding sLORETA image. The rationale for presenting the number of active voxels was to obtain a measure of temporal dynamic activity of each structure. The brain structures of interest included those found active in MI and HLT experiments (Decety et al., 1994; Vingerhoets et al., 2002).

To find the predominantly active areas on the cortex for HLT and MI, the sLORETA statistical package was used to perform a paired group analysis ($n=15$) for HLT and MI trials where a pair comprises

the baseline window and a selected one second window. Paired group analysis was also performed to compare the differences in spatial activation and activation intensity between MI and HLT types. Using sLORETA's log of ratio of averages (r-value) for the first test and *t*-statistics (*t*-value) for the second test, 5000 randomisation of statistical non-parametric mapping (SnPM) (Nichols & Holmes, 2002) implemented in sLORETA package was used to calculate corrected critical thresholds and p-values. Statistical significant level was set at $p=0.05$.

3. Results

3.1. Behavioural data

The mean RTs and accuracies are presented in Table 1. The mean RT across all subjects and trials for the right hand CCW was 1427 ± 493 ms (MEAN $\pm$ STD), for the left hand CW it was 1549 ± 500 ms, for the right hand CW it was 1613 ± 554 ms and for the left hand CCW it was 1638 ± 551 ms. For these RTs, the two-way ANOVA revealed main effects for hand pictures, $F(1,14)=6.163$, $p=0.026$ and picture orientations $F(1,14)=6.475$, $p=0.023$ and significant interaction of hand pictures $\times$ picture orientations, $F(1,14)=14.068$, $p=0.002$. The interaction was significant because the right hand pictures were recognised significantly earlier at CCW orientation than at CW orientation and left hand pictures were recognised significantly earlier at CW orientation than at CCW orientation.

These results showed that the medial orientations (right hand CCW and left hand CW) had the lowest RTs. The RT results were comparable with those from the published literature (Takeda et al., 2010; Cooper & Shepard, 1975), although in the referenced studies participants provided their response by pressing a button rather than by giving a verbal response. The accuracy rates (100% – % error rate) had medians of 97, 97 93 and 93% for left CW, right CCW, left CCW and right CW respectively. There were no statistically significant differences in median accuracy between the hand pictures ($z=0.1343$, $p=0.8931$) and picture orientations ($z=-0.1418$, $p=0.8872$). There was also no statistically significant difference in median accuracy between the lateral (right CW+left CCW) and the medial (right CCW+left CW) orientations ($z=-0.8359$, $p=0.4032$).

Table 1
Mean RTs and accuracies for each subject and condition.

Subjects	RT (ms)				Accuracy (%)			
	Left CW	Right CCW	Left CCW	Right CW	Left CW	Right CCW	Left CCW	Right CW
1	1833	1647	1881	1879	95	97	97	92
2	1604	1381	1798	1770	92	97	92	90
3	1816	1453	1688	1754	97	98	95	100
4	1415	1099	1527	1441	83	85	85	93
5	1122	953	1253	1212	80	78	75	58
6	1482	1378	1511	1500	98	98	93	100
7	1669	1552	1660	1454	95	98	93	97
8	1515	1672	1761	2023	87	93	88	87
9	1312	1253	1375	1364	98	100	100	100
10	1633	1751	1785	1763	97	92	93	87
11	1799	1732	1850	1909	97	100	92	92
12	1004	933	1100	1038	100	97	100	100
13	1417	1406	1528	1393	100	93	100	95
14	1546	1416	1546	1515	100	100	100	97
15	2346	1820	2918	2540	76	72	62	66

3.2. Time-frequency analysis in EEGLAB

Although medial and lateral RTs were significantly different, no statistically significant difference was found between the corresponding ERD/ERS maps. However because the RTs were different between the two orientations, their data were not merged to avoid disrupting the temporal pattern of events in each orientation. Therefore, only the results for the medial orientations will be presented for the HLT. Average ERD/ERS maps of two channels C3 and C4 located over the sensorimotor areas (one from each hemisphere) are plotted in Fig. 4 to show time-frequency dynamics. The plot is presented from the moment when the execution cue appeared on the computer screen. ERD is shown with negative values while ERS is shown with positive values. The last column presents the area of statistical significant differences (shaded area) in ERD/ERS between MI and HLT in frequency and time. The last row presents the area of statistical significant differences in ERD/ERS between the right and left hand. The plot at the bottom right shows the area of statistical interactions between tasks and conditions.

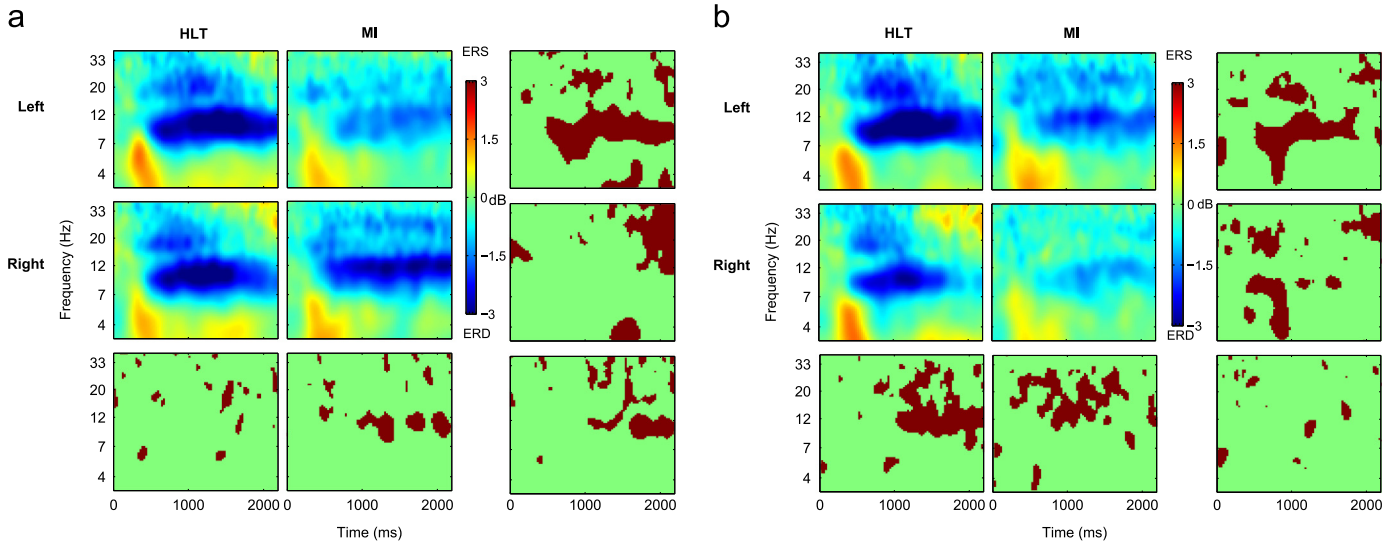

Fig. 4. ERD/ERS maps over electrode location (a) C3 and (b) C4 averaged across all subjects for MI (left and right) and HLT (left CW and right CCW). The relevant period and frequency band ($t=0$–2200 ms and 3–40 Hz) are shown. ERD is shown with negative values while ERS is shown with positive values. The last columns show the area of statistical differences between the corresponding two conditions in frequency and time ($p=0.05$ with Holm's correction for multiple comparison). The last row represents the area of statistical differences between the right and left hand. The plot on the bottom right represents the statistical interactions between the conditions and their left and right types.

The ERS at around 300 ms is related to visual processing of the execution cue. At about 500 ms, ERD is seen for all conditions in the α/μ, $\beta1$ and $\beta2$ frequency bands. The intensity of ERD is in general lateralised with the right hand being more intense on C3 and the left hand on C4. In the case of MI, left and right hand ERD differences (see the second map on the last row of Fig. 4b) emerge early at approximately 500 ms and it is more prominent on channel C4.

For the HLT, a close inspection of the ERD/ERS of the right and left hand and the corresponding statistical difference maps show that its ERD can be separated into an early and a late ERD. The early ERD is the HLT ERD occurring between 500 to about 1000 ms while late ERD is the HLT ERD starting from about 1000 ms. Observing RT, early ERD can be said to occur long before laterality judgement was made while the late ERD started just before and after laterality judgement was made. This late and early ERD effect is more prominent on channel C4. The early ERD is not significantly different between the left and the right hand, as shown by the map on the bottom left of Fig. 4b. However, the late ERD is significantly different between HLT of the left and right hand, indicating that it is hand specific.

The ERD of MI is significantly different between left and right hand throughout the whole period, being hand specific from the onset of ERD at $t=500$ ms. The late ERD in HLT is similar to that of MI of the corresponding hand especially in the $\beta1$ and $\beta2$ bands. The ERD for the HLT tends to decrease after verbal response. This may have created the differences between HLT and MI towards the end of the trials because subjects continued MI until the end of the trials. The statistical interactions between the conditions and types are only more profound in the later part at C3 in the α/μ frequency band.

The scalp distribution of the ERD/ERS in α/μ, $\beta1$ and $\beta2$ frequency bands are shown in Fig. 5. The scalp map was obtained for the time window 1000–1200 ms which is a time window including the late ERD. This time window is prior to the fastest RT (1427 ms) and therefore should have a reduced interference from the verbal response. The last columns highlight channels/electrodes that show statistically significant differences in ERD/ERS between the corresponding two conditions (left HLT and left MI in the first rows, right HLT and right MI in the second rows for a chosen frequency band) while the last rows show the differences between the right and left hand. The plot on the bottom right shows the statistical significant interactions between HLT, MI, left and right. Differences between MI and HLT task will be analysed first. At the chosen time window most of the ERD/ERS differences between right hand MI and right CCW HLT appear in the posterior parietal and occipital channels showing that their ERD/ERS in the sensorimotor areas are comparable in the α/μ, $\beta1$ and $\beta2$ frequency bands. In the case of the left hand MI and left CW HLT, the difference is widespread including the motor areas in the α/μ band but in the $\beta1$ and $\beta2$ bands the differences is concentrated on the parietal and on the occipital areas. The absence of significant differences on the frontal and paracentral areas shows a comparable intensity of activation of the sensorimotor areas during MI and HLT. When ERD scalp maps were compared between the left and right hand significant differences can be seen in all the three frequency bands for MI but predominantly in the $\beta1$ and $\beta2$ bands in HLT. For MI, areas of statistical significant difference between left and right hand include dominantly the right parietal and central channels including C4. Because the late ERD in HLT is hand specific and therefore resembles the ERD of MI, areas of statistically significant difference between two hands are similar to those of MI.

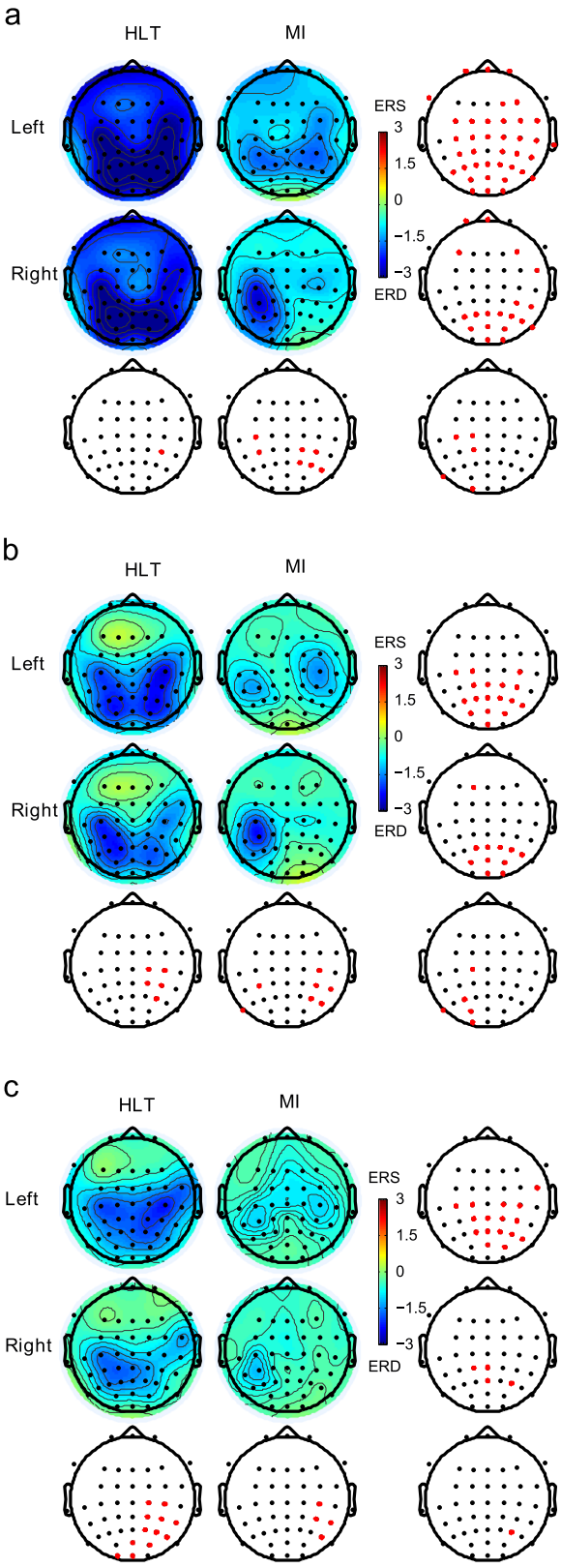

Fig. 5. Scalp maps of ERD/ERS in different frequency bands at 1000-1200 ms post cue for MI (left and right) and HLT (left CW and right CCW). ERD is shown with negative values while ERS is shown with positive values. The last columns highlight channels/electrodes that show statistical difference between the corresponding two conditions ($p=0.05$ with Holm's correction for multiple comparison) while the last rows show the same for the difference between the right and left hand. The plot on the bottom right represents the statistical interactions between the conditions and their types. (a) α/μ, 8–12 Hz. (b) $\beta1$, 12–16 Hz. (c) $\beta2$, 16–24 Hz.

3.3. sLORETA localisation

Changes in the cortical activation of relevant brain structures over time were expressed as a function of the number of active voxels in

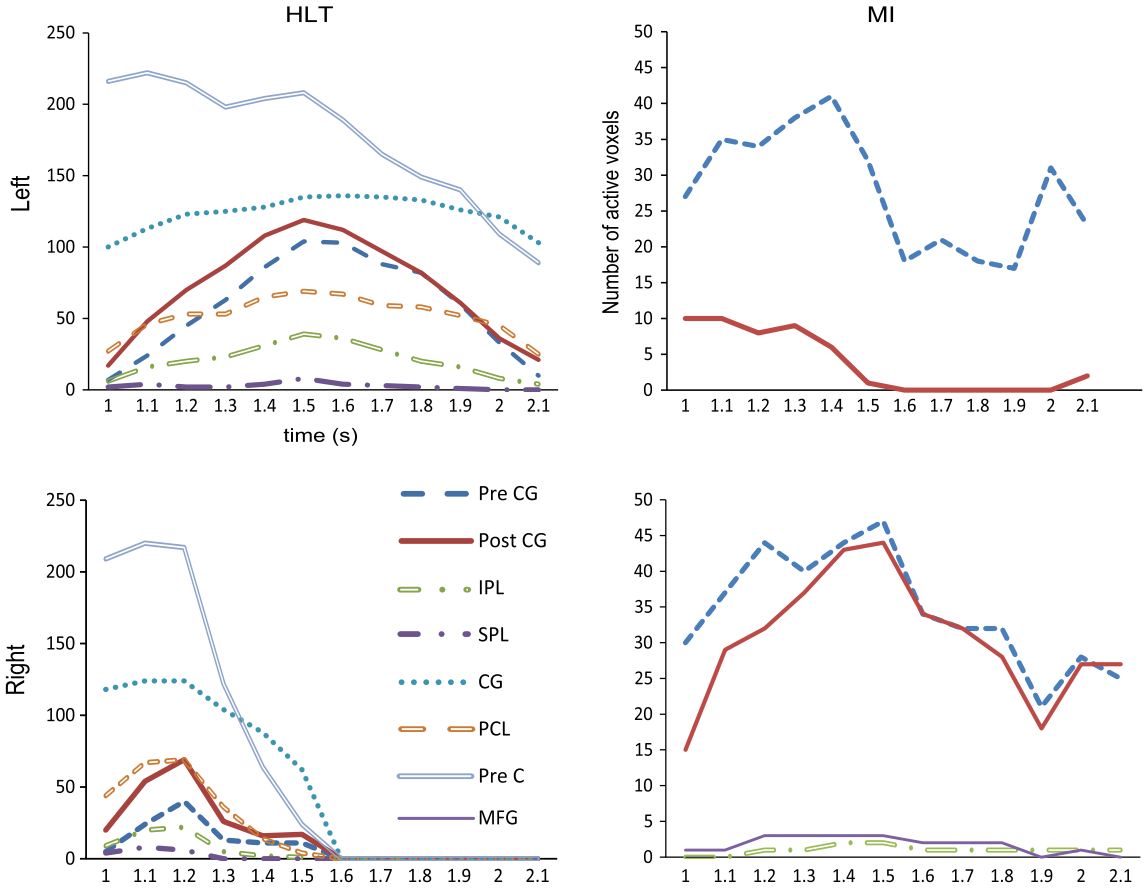

Fig. 6. Temporal activation pattern of cortical structures in the α/μ–band of sLORETA localisation for MI (left and right) and HLT (left CW and right CCW). The number of active voxels was counted for each cortical structure for each sLORETA image computed in a one second sliding window with a step size of tenth of a second. The time axis represents the centres of the one second sliding windows. Pre CG, Precentral gyrus; Post CG, Postcentral gyrus; IPL, Inferior Parietal Lobule; SPL, Superior Parietal Lobule; CG, Cingulate gyrus; PCL, Paracentral lobule; Pre C, Precuneus; MFG, Middle Frontal Gyrus.

different time windows. Different experimental condition showed distinctive temporal variations of the cortical activity. Temporal activation of representative structures is shown in Fig. 6. The HLT had larger number of active voxels and larger temporal variation than MI. Selected brain regions reached their maximum activity fastest for the right hand CCW where the activities plateaued at the time window t=700–1700 ms. For left CW the plateau was within the time window t=1000–2000 ms and for both the right CW and left CCW (not shown on the figure) it was within the window t=1100–2100 ms with temporal distribution similar to that of left CW HLT. The time window used for sLORETA analysis in which plateaus occurred corresponds to the time window as their respective RTs, apart from the plateau for the right CCW which had significantly shorter RT. Compared to HLT the number of voxels during MI was less variable over time (note the different time scales for HLT and MI). In both MI and HLT there are clear activities of the postcentral gyrus and precentral gyrus and the plateaus in the case of HLT are possibly related to the maximum activity occurring during implicit MI. The IPL and the middle frontal gyrus were active for the right hand MI but did not reach the significance level (p=0.05) in the case of the left hand MI. The cingulate gyrus and the paracentral lobule were also activated in HLT.

The rest of sLORETA results will be presented as follows. sLORETA images and the corresponding tables of activities will be presented for each of the four conditions in Fig. 6 (i.e. left hand MI, right hand MI, left CW HLT and right CCW HLT) in order to individually describe each condition. Afterwards, an sLORETA image and corresponding table of activities will be presented for the comparison between right hand MI and the right CCW HLT to further show the similarities and differences between MI (explicit MI) and HLT (implicit MI).

In order to present a sLORETA image that best describes each of the conditions' sensorimotor activities, sLORETA images corresponding to a condition's specific plateau time window of the sensorimotor area is presented. Assuming that in the case of MI, the number of active voxels were relatively constant, the time window t=500–1500 ms was chosen to present MI images.

As it can be seen from Figs. 7 and 8 the right and left hand MI engendered strong activation contralaterally. Active regions are summarised in Tables 2 and 3 for the right and left hand MI respectively. The sLORETA images are presented for the right CCW HLT in Fig. 9 and for the left CW HLT in Fig. 10. The activities in the α/μ band were significant for both conditions; those in the β1 frequency band were significant in the case of MI but not in the case of HLT. The sLORETA localisation for MI in the β1 band is similar to that in the α/μ band, therefore unless otherwise specified the α/μ localisation for MI is referred. The activities in the β2 frequency band did not reach significance level in any condition. In both MI and HLT the postcentral gyrus, the precentral gyrus and IPL (BA 40) and the middle frontal gyrus were always active. For HLT the activities of these structures were bilateral with the strongest active voxel contralateral to the chosen hand. The medial frontal gyrus active during mental rotation task (Gogos et al., 2010) and the paracentral lobule part of the frontal and the parietal lobe were also active in HLT. Like in other neuroimaging studies on mental rotation (Zacks, 2008), SPL and IPL were always active bilaterally for all types of HLT. The cingulate gyrus, posterior cingulate and the precuneus which has been referred metaphorically to as the mind's eye

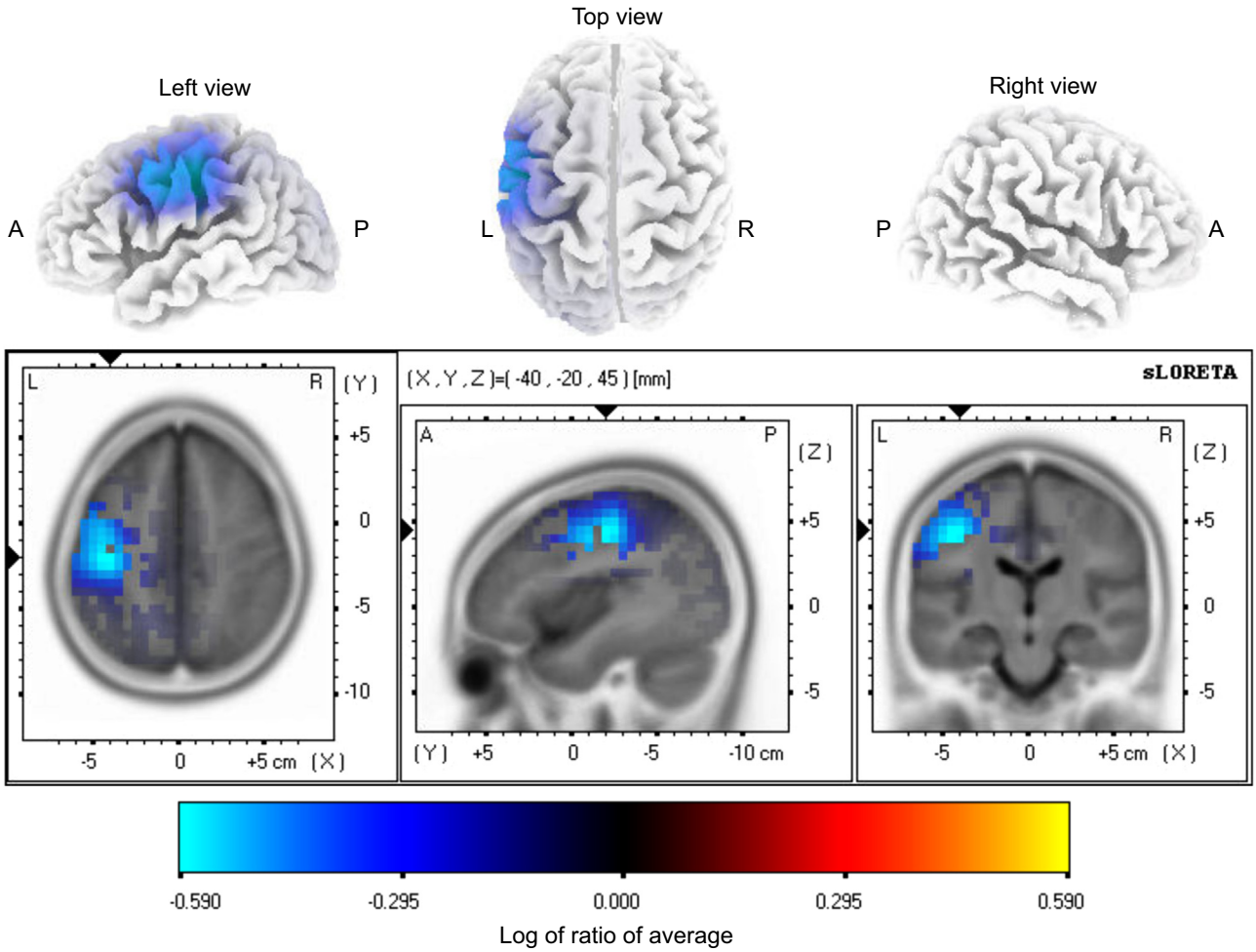

Fig. 7. sLORETA localisation for MI of right hand compared with the baseline period in the α/μ–band at the time window 500–1500 ms relative to execution cue onset. The first row shows 3D map of the localisation while the second row shows a 3D slice at the displayed location (BA 4). The localisation for the β1-band is similar to that of α/μ and therefore it is not shown here.

(Fletcher et al., 1995) were particularly active. In the occipital cortex, the notable active areas included the cuneus, middle occipital gyrus and the lingual gyrus. The activities found in the auditory cortex namely the superior temporal gyrus and the transverse temporal gyrus might have been due to the beep sound used in the HLT trials although the superior temporal gyrus has been found active in a mental rotation task (Gogos et al., 2010). There were also activities in the insula and the parahippocampal gyrus. These and other active areas are summarised in Tables 4 and 5 for the right CCW and the left CW respectively.

The results of comparing cortical activity between MI and HLT are presented for the right hand MI versus right CCW HLT in Fig. 11 and in Table 6. There were no differences between the conditions in the hand areas of the precentral gyrus and the postcentral gyrus, indicating similarities in the intensity of activation in these areas in both conditions. As expected there were more activities in the SPL in HLT than in MI. Other areas more active during HLT included the central areas, the precuneus and the sub-gyral. Similar results to those presented were also obtained by comparing left hand MI with left CW HLT, right hand MI with right CW HLT and left hand MI with left CCW HLT.

4. Discussions

It is believed that mental rotation of hand involves MI implicitly. Using time-frequency decomposition methods, EEG recorded during mental rotation tasks was studied with three main objectives. First to understand the dynamics of sensorimotor activity during mental rotation induced by HLT. Second, to investigate if it is possible to discriminate between left and right hand mental rotation exploiting the time frequency technique. The third was to compare temporal dynamic activation of the sensorimotor cortex during implicit and explicit MI across different frequency bands.

In the first objective, the time frequency analysis of EEG signal recorded during HLT showed activities in the α/μ frequency band and in the β (β1 and β2) bands . Similar frequency bands showed ERD activities in previous mental rotation studies using 3D objects and hands (Riečansky` & Katina, 2010; Gill et al., 1998; Chen et al., 2013). Activities in these frequency ranges are believed to show spatiotemporal patterns in motor, and cognitive tasks (Neuper & Pfurtscheller, 2001; Neuper, Wörtz, & Pfurtscheller, 2006; Crone et al., 1998) such as HLT. The maximum α/μ ERD in HLT was localised on the sensorimotor, posterior parietal and the occipital areas although this ERD was not spatially specific. The activities in about 8–12 Hz band in the posterior parietal and the occipital area during mental rotation (Michel, Kaufman, & Williamson, 1994) might have a global effect and therefore contribute to this non-spatial specificity. The 8–12 Hz band activities might influence α/μ activities recorded in the sensorimotor areas although we used the common average method of electrode derivation to enhance local activities. In the case of the β bands in HLT, activity was more transient and spatially specific in accordance with the characteristics of motor related ERD in the β band (Crone et al., 1998). These β ERDs

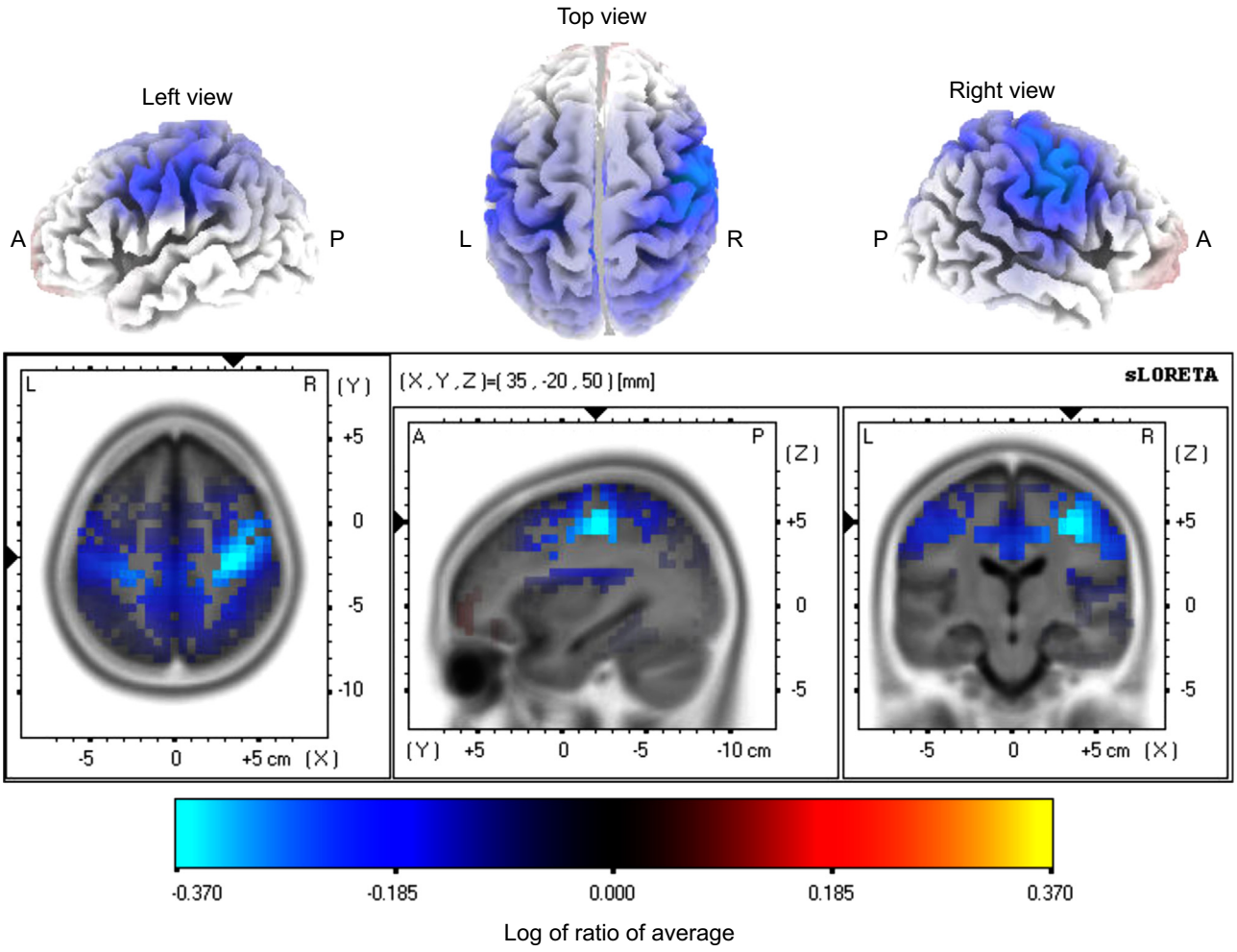

Fig. 8. sLORETA localisation for MI of left hand compared with the baseline period in the α/μ–band at the time window 500–1500 ms relative to execution cue onset. The first row shows 3D map of the localisation while the second row shows a 3D slice at the displayed location (BA 4). The localisation for the β1-band is similar to that of α/μ and therefore it is not shown here.

Table 2
Significantly active structures for right hand MI compared with the baseline period in α/μ–band and β1-band obtained at time window 500–1500 ms relative to cue onset.

F	Structure	BA	H	nv	Voxel with max. *r*-value			
					r-value	*x*	*y*	*z*
α/μ	Postcentral gyrus	2 ***3***	L	15	−0.59	−45	−18	38
	Precentral gyrus	***4*** 6	L	30	−0.59	−40	−17	42
	Middle frontal gyrus	***6***	L	1	−0.54	−45	2	41
β1	Postcentral gyrus	***3*** 2	L	29	−0.63	−40	−22	43
	Precentral gyrus	***4*** 6	L	10	−0.62	−40	−17	42
	Inferior parietal lobule	***40***	L	1	−0.54	−50	−27	43

Notes: The structures are sorted in the descending absolute values of r-value. F, Frequency band; BA, Brodmann Area; H, Hemisphere; nv, Number of Voxels; r-value, Statistics (log of ratio of averages implemented in sLORETA, read like *t*-values); xyz, Talairach coordinates; R, Right; L, Left. The BA in bold font is the Brodmann area whose coordinate is displayed. The BA in italics is the Brodmann area contributing most in nv. The H in bold font is the hemisphere that contributes more than 20% of nv.

Table 3
Significantly active structures for left hand MI compared with the baseline period in the α/μ–band and β1-band at the time window 500–1500 ms relative to cue onset

F	Structure	BA	H	nv	Voxel with max. r-value			
					r-value	x	y	z
α/μ	Precentral gyrus	***4*** 6	R	27	−0.37	35	−17	47
	Postcentral gyrus	***3***	R	10	−0.37	35	−22	47
β1	Precentral gyrus	***4*** 6	R	7	−0.35	35	−17	42

Notes: See Table 2.

were localised over the sensorimotor and posterior parietal areas. Temporally the ERD in all the frequency bands began at approximately $t=500$ ms and diminished soon after the subjects' verbal responses measured by RT. These results suggest that the sensorimotor activities quantified with ERD during mental rotation of hands can be studied in the chosen frequency bands. sLORETA localisations in the α/μ band confirmed that structures in the sensorimotor areas contributed to the ERD activities. Furthermore the sLORETA localisations showed that the activation of the sensorimotor areas peaked at different times for each hand and picture orientations during the trials. Apart from the right CCW HLT, where the peak activity in sLORETA occurred about 200 ms earlier than RT, the mean RTs closely followed the times of peak sensorimotor activity (because RTs occurred in the same time window as the corresponding sensorimotor peak activity). This means that the time of sensorimotor peak activity corresponds to the RT, being faster for medial than for lateral orientation. According to Parsons (Parsons, 2001; Moseley et al., 2012),when a person is presented with a HLT, the person makes an initial spontaneous pre-conscious judgement which is subsequently

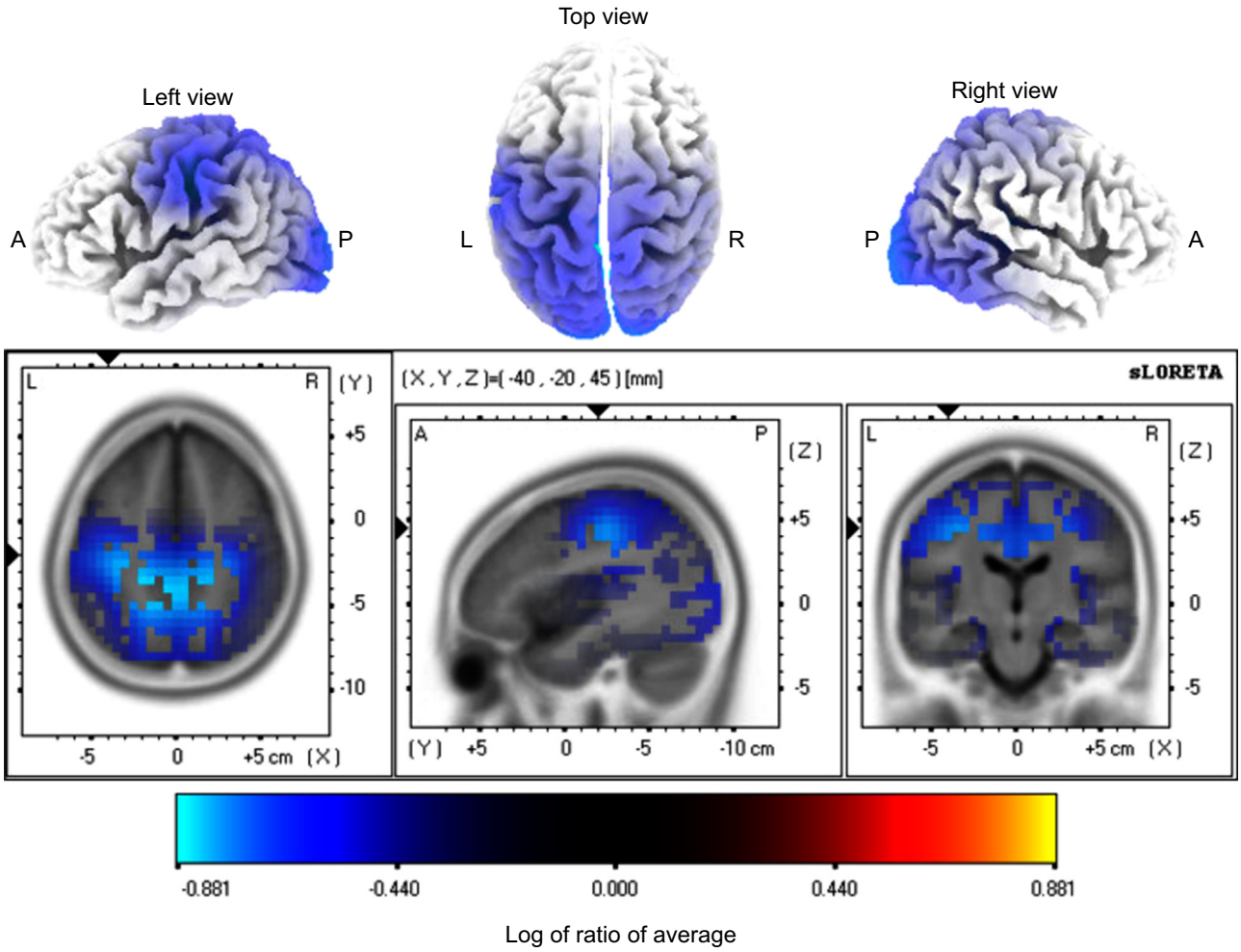

Fig. 9. sLORETA localisation for right CCW HLT compared with the baseline period in the α/μ−band at the time window 700–1700 ms relative to execution cue onset. The first row shows 3D map of the localisation while the second row shows a 3D slice at the displayed location (BA 4). The localisation for the β1-band is similar to that of α/μ but it was not statistically significant.

confirmed by an implicit MI of the hand implicated in the pre-conscious judgement. It is possible that the pre-conscious judgement was biased towards the right hand given that the subjects were right-handers. This would imply that the first confirmation process involving implicit MI was biased towards the right hand. So given a right hand image in a medial orientation, this first confirmation process was often successful. This might explain the early peak activity for the right CCW HLT although it does not explain why its mean RT occurred at about 200 ms after the peak activity.

For the second objective, statistical analysis of ERD/ERS showed that there were differences between left and right mental rotation induced by HLT. The differences could only be observed during the late ERD phase in HLT, 1000 ms after the execution cue. Hemispheric differences could be observed with the late ERD but not with the early ERD. This explains why a previous EEG study did not report any hemispheric difference between left and right HLT (Chen et al., 2013). In the case of MI the left and right hands' ERD differences started at the onset of ERD ($t=500$ ms). Discrimination between left and right hand MI has been exploited in brain computer interface (Pfurtscheller et al., 2006; Enzinger et al., 2008; Wolpaw, Birbaumer, McFarland, Pfurtscheller, & Vaughan, 2002). The results of this study suggested that the discrimination can also be achieved with data recorded during HLT. Furthermore, similar electrode locations can be used for this discrimination for both MI and HLT. With regard to sLORETA localisations, there were no quantitative differences between the left and right hand mental rotation although there were stronger activations in the contralateral hemisphere to the presented hand. There was also no difference between left and right hand MI in sLORETA analysis despite differences being present in the channel based time frequency analysis. Vingerhoets and colleagues faced a similar issue in an fMRI study (Vingerhoets et al., 2002) on mental rotation. As suggested in the Vingerhoets' study activities in the ipsilateral hemispheres to each hand were sufficient to neutralise the lateralised activities when both hands data were contrasted.

For the third objective, ERD/ERS was compared between MI (explicit MI) and HLT (implicit MI). There were similarities between the two conditions in the later part of the trials when the late ERD occurred. The similarities were present in the sensorimotor areas. The results also showed that MI and HLT mainly differ in the activation of the posterior parietal and occipital regions where ERD activation intensity was stronger for HLT. The frequency bands that best described the similarities between MI and HLT were the β1 and β2. The α/μ band in the case of HLT was not spatially specific although its maximum was on the sensorimotor, parietal and occipital areas.

The sLORETA localisation of MI resembles those obtained in a study by Dyson and colleagues (Dyson, Sepulveda, & Gan, 2010) who localised cortical activities during explicit MI. All of the structures active during MI were active during HLT. These structures included the precentral gyrus, postcentral gyrus, IPL and the middle frontal gyrus (BA 6). This result supports the propositions in the literatures that MI is used during mental rotation (Vingerhoets et al., 2002; Cooper

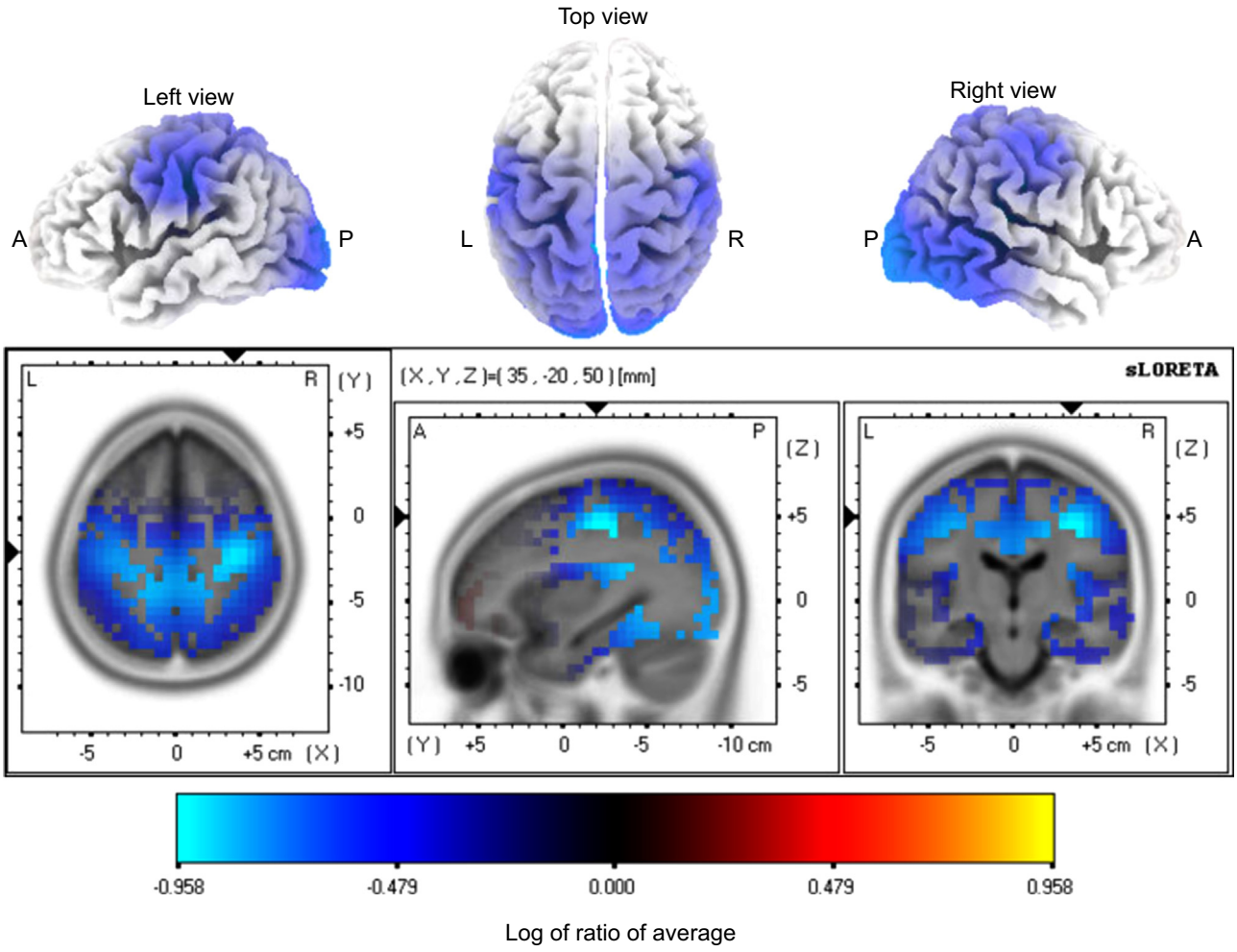

Fig. 10. sLORETA localisation for left CW HLT compared with the baseline period in the α/μ–band at the time window 1000–2000 ms relative to execution cue onset. The first row shows 3D map of the localisation while the second row shows a 3D slice at the displayed location (BA 4). The localisation for the β1-band is similar to that of α/μ but it was not statistically significant.

Table 4
Significantly active structures for right CCW HLT compared with the baseline period in α/μ–band at the time window 700–1700 ms relative to cue onset.

F	Structure	BA	H	nv	Voxel with max. *r*-value			
					r-value	*x*	*y*	*z*
α/μ	Cingulate gyrus	***31***	R L	124	−0.88	−10	−42	34
	Precuneus	***31*** 7	R L	217	−0.88	−5	−47	30
	Posterior Cingulate	***30***	R L	87	−0.87	5	−47	25
	Sub-gyral	***31*** 7	R **L**	14	−0.86	−20	−47	35
	Cuneus	***18***	R L	237	−0.83	15	−67	17
	Paracentral lobule	***31*** 5	R L	69	−0.82	0	−32	43
	Postcentral gyrus	***3***	R **L**	69	−0.81	−30	−22	43
	Lingual gyrus	***18***	R L	165	−0.81	20	−53	7
	Precentral gyrus	***4*** 6	R **L**	40	−0.79	−25	−27	47
	Parahippocampal gyrus	***19***	**R** L	56	−0.79	20	−48	2
	Insula	***13***	**R** L	15	−0.79	30	−33	20
	Inferior parietal lobule	***40***	R **L**	22	−0.79	−35	−32	38
	Middle occipital gyrus	***18*** 19	**R** L	56	−0.75	−15	−87	14
	Superior temporal gyrus	***41***	R	3	−0.74	35	−33	15
	Superior parietal lobule	5 ***7***	R **L**	6	−0.73	−25	−51	44
	Medial frontal gyrus	***6***	R L	9	−0.72	10	−22	47
	Fusiform gyrus	***19***	R	35	−0.71	25	−54	−10
	Inferior occipital gyrus	***18***	**R** L	11	−0.71	30	−92	−4
	Transverse temporal gyrus	***41***	R	2	−0.68	40	−33	11
	Middle frontal gyrus	***6***	L	2	−0.67	−35	−8	42

Notes: See Table 2.

& Shepard, 1975; Parsons, 1987a, 1987b, 1994; Parsons et al., 1995; Wexler et al., 1998) and suggests that implicit MI is similar to explicit MI. In the case of MI the statistically significant active sensorimotor areas were completely lateralised while for the HLT they were bilateral possibly because the late and early ERD both occurred within the long-time window analysed in sLORETA. However the strongest active voxel in the sensorimotor areas for HLT was always contralateral to the hand chosen by the subjects. The activities in the β1 frequency band were found significantly active for the MI but it did not reach significance level in the HLT condition. This was attributed to the excessive energy in the α/μ band in HLT which dominated the activities in the β bands following the correction for multiple comparisons over all frequency bands. When the α/μ band was excluded from the analysis the β band became significant.

Comparing HLT and MI data in sLORETA did not reveal any statistical significant difference in the sensorimotor cortex of the hand suggesting that these areas were similarly active in both conditions. Instead, as expected the SPL, active in mental rotation tasks (Vingerhoets et al., 2002), and other areas in the parietal cortex were among the areas showing higher activation in HLT than in MI condition. Some previous studies have suggested that the primary sensorimotor cortices are not active during HLT unlike during MI (Parsons, 2001; Moseley et al., 2012). The absence of any difference in primary sensorimotor activity between the two conditions might be due to the EEG methodology used in this

Table 5
Significantly active structures for the left CW HLT compared with the baseline period in the α/μ–band at the time window 1000–2000 ms relative to cue onset.

F	Structure	BA	H	nv	Voxel with max. *r*-value			
					r-value	*x*	*y*	*z*
α/μ	Postcentral gyrus	***3***	R L	119	−0.96	35	−22	43
	Precentral gyrus	***4*** 6	R L	104	−0.96	35	−17	42
	Sub-gyral	***2*** *7*	R **L**	19	−0.93	35	−27	38
	Cingulate gyrus	***31***	R L	135	−0.93	20	−42	25
	Precuneus	**31** *7*	R L	208	−0.93	20	−42	30
	Posterior Cingulate	**23** *30*	R L	87	−0.92	5	−42	25
	Lingual gyrus	***18***	R L	180	−0.91	20	−53	7
	Insula	***13***	**R** L	31	−0.89	30	−33	20
	Parahippocampal gyrus	***19***	**R** L	81	−0.89	20	−48	2
	Cuneus	**30** *18*	R L	250	−0.88	10	−58	8
	Paracentral lobule	**31** *5*	R L	69	−0.86	0	−32	43
	Inferior parietal lobule	***40***	R L	39	−0.85	40	−32	34
	Superior temporal gyrus	***41***	R	22	−0.85	35	−33	15
	Fusiform gyrus	**19** *37*	**R** L	100	−0.83	25	−54	−10
	Middle frontal gyrus	***6***	R L	11	−0.83	35	−8	42
	Middle occipital gyrus	***18***	**R** L	107	−0.82	30	−92	5
	Inferior occipital gyrus	***18***	**R** L	20	−0.81	30	−92	−4
	Transverse temporal gyrus	***41***	R	5	−0.81	40	−33	15
	Supramarginal gyrus	***40***	R	3	−0.79	40	−42	34
	Middle temporal gyrus	***37***	R	52	−0.78	45	−58	−1
	Medial frontal gyrus	***6***	R L	11	−0.77	10	−22	47
	Inferior temporal gyrus	***37***	R	27	−0.76	45	−68	−1
	Superior occipital gyrus	***19***	R	2	−0.74	30	−86	23
	Superior parietal lobule	5 ***7***	R L	8	−0.74	25	−51	44

Notes: See Table 2.

study. Its disadvantage lies in the low spatial resolution in which neighbouring cortical structures may have correlated activity. However it could be that the EEG method which offers highly resolved time-frequency analysis may be more sensitive to transient changes. This was demonstrated by the temporal dynamics of the activities of cortical structures which peaked at certain times during HLT.

4.1. Other active areas in HLT

A literature review on mental rotation reported that activities were wide spread over several brain areas (Zacks, 2008; Gill et al., 1998; Cohen et al., 1996; Jordan et al., 2001). The only areas consistently reported in all studies were the SPL and the intraparietal sulcus and similar areas were presented in the current study. The other areas mostly reported in mental rotation or related tasks which were also reproduced by sLORETA in this study included the following. The insula cortex (Zacks, 2008; Wraga et al., 2003), found active during voluntary hand movement (Fink, Frackowiak, Pietrzyk, & Passingham, 1997), was consistently active. The precunues (BA 5 and 7) which has been implicated in self centered mental imagery (Cavanna & Trimble, 2006) and other parietal areas were major active areas (Cohen et al., 1996; Zacks, 2008). In the limbic lobe the cingulate gyrus and the posterior cingulate cortex were prominently active in all types of HLT conditions (Wraga et al., 2003). The posterior cingulate cortex has previously been found active in attention requiring tasks (Leech, Braga, & Sharp, 2012) and

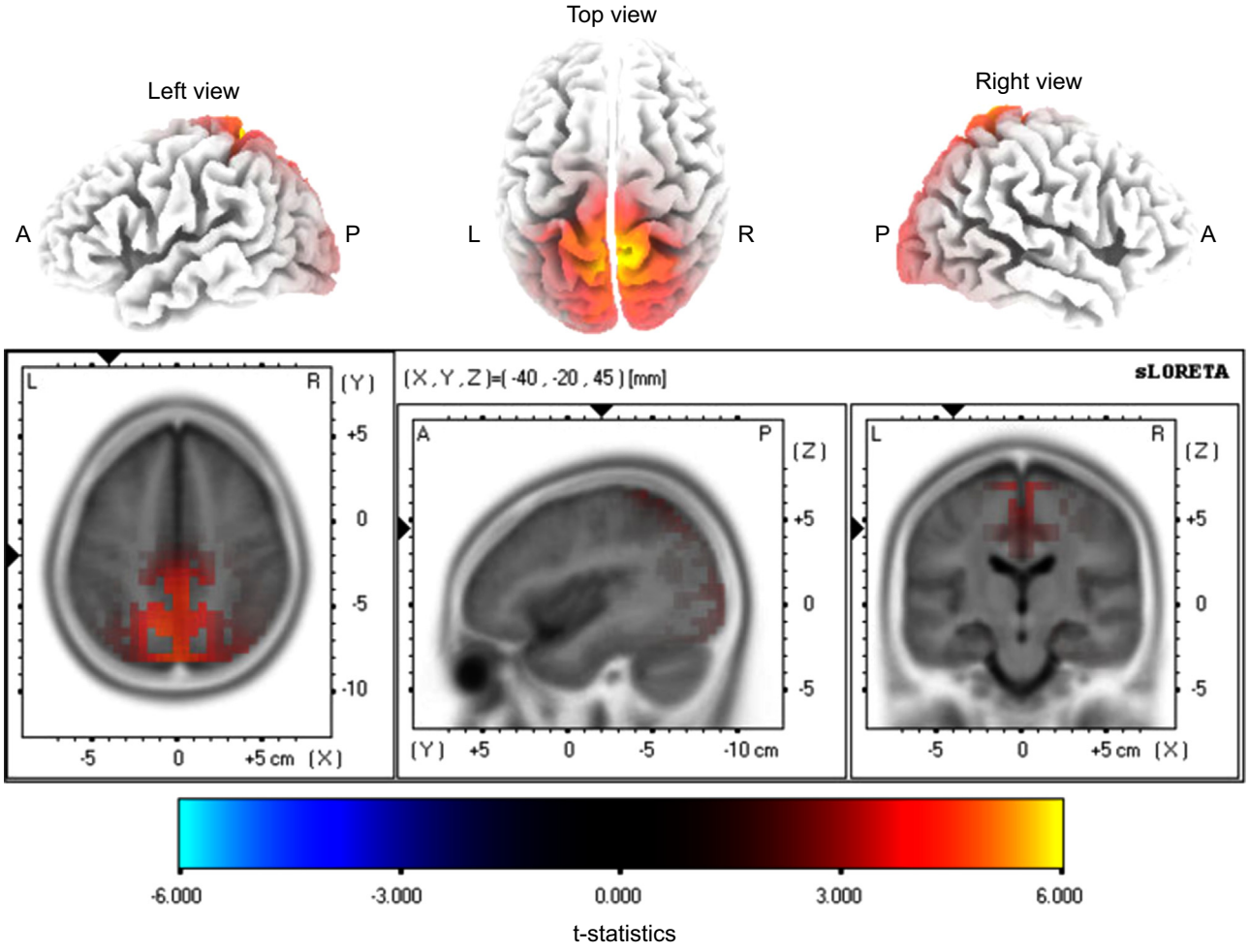

Fig. 11. sLORETA localisation of the differences between the right hand MI and the right CCW HLT in the α/μ–band at the time window 500–1500 ms. In all the presented areas (red), HLT is more active than MI. The first row shows 3D map of the localisation the second row shows a 3D slice at the displayed location (BA 4). The localisation for the β1-band is similar to that of α/μ but it was not statistically significant. (For interpretation of the references to colour in this figure caption, the reader is referred to the web version of this paper).

Table 6
Structures with significant differences in activity between right hand MI and right CCW HLT in α/μ−band at time window t=700–1700 ms. In all the presented structures, HLT is more active than MI.

F	Structure	BA	H	nv	Voxel with max. t-value			
					t-value	x	y	z
α/μ	Postcentral gyrus	***5***	R L	46	5.90	5	−45	67
	Paracentral lobule	***5***	R L	58	5.61	5	−45	62
	Precuneus	***7*** 19	R L	125	5.48	0	−50	62
	Superior parietal lobule	***5*** 7	**R** L	28	4.62	−20	−41	62
	Medial frontal gyrus	***6***	R L	8	4.40	0	−26	57
	Precentral gyrus	***4***	R **L**	3	4.37	−15	−31	66
	Cingulate gyrus	***31***	**R** L	4	4.35	5	−42	44
	Sub-gyral	***7***	L	1	4.13	−20	−46	53

Notes: See Table 2.

in visual mental imagery (Kosslyn et al., 1993). In the temporal lobe, activities were found in the posterior temporal cortex (BA 37 including the fusiform gyrus) (Alivisatos & Petrides, 1996; Jordan, Heinze, Lutz, Kanowski, & Jäncke, 2001; Kosslyn et al., 1993; Gill et al., 1998) and the parahippocampal gyrus. The parahippocampal gyrus is known to play a part in the memory encoding and retrieval. It has also been implicated in the encoding and recognition of scenes (Epstein & Kanwisher, 1998). In the occipital lobe there were activities in the cunues (Wraga et al., 2003), the fusiform gyrus (BA 19) which has overlapping areas that respond to faces (Kanwisher, McDermott, & Chun, 1997) and body parts (Schwarzlose, Baker, & Kanwisher, 2005). Other areas included the lingual gyrus, the superior, middle, and the inferior occipital gyri. (Vingerhoets et al., 2002; Jordan et al., 2001; Gogos et al., 2010; Weiss et al., 2009).

4.2. EEG and sLORETA tomography

While being spatially less accurate than fMRI and PET, EEG is suitable for analysing extracellular electrical field potentials recorded from the scalp with miliseconds resolution in different frequencies which is important in studying dynamic processes in the brain (Mulert et al., 2004). It is a measure of neuronal electrical activity and not hemodynamic response, the later having latency between a task and the related brain activity. The ERD/ERS method can reveal time-frequency characteristics of cortical processes but it cannot ascertain precise location of that activity; furthermore it can provide spatially averaged activity over the surface of the cortex only. Multiple EEG sources can be simultaneously localised using source localisation tool such as sLORETA at the expense of low spatial resolution. Given this sharp resolution, neighbouring neuronal sources in the sLORETA localisations will be highly correlated but fMRI and PET studies have produced similar localisations as those presented in this study. It is important to point out that sLORETA has been extensively validated and found to have no localisation bias (Pascual-Marqui, 2007; Sekihara et al., 2005; Greenblatt et al., 2005). A previous version (Pascual-Marqui, Michel, & Lehmann, 1994) has already been validated with fMRI (Mulert et al., 2004; Vitacco et al., 2002), structural MRI (Worrell et al., 2000), and PET (Dierks et al., 2000; Pizzagalli et al., 2003; Zumsteg, Wennberg, Treyer, Buck, & Wieser, 2005).

4.3. Shortcomings

A possible shortcoming of the study is that the results were derived from only 15 young healthy individuals and therefore might not reflect a general case. Also it was not possible to determine whether the HLT and the MI task were of equal difficulty. However, the chosen orientation of the pictures especially the medial orientations were relatively natural to the hands so the HLT was not expected to be more difficult than MI of movement in a similar orientation as the medial and lateral orientations.

5. Conclusions

During the hand mental rotation task, the recorded brain activity had similar spatial and time-frequency characteristics to those found during explicit motor imagery. The sensorimotor activity is known to be distinctive for left and right hand explicit MI. It was shown here that the sensorimotor activity was also distinctive for the left and right hand mental rotation. These suggest that implicit MI used during the mental rotation of hand in HLT is similar to explicit MI. These results indicate that mental rotation of body parts can be used to complement MI in areas of rehabilitation in which MI is used for therapeutic purposes. Patients who are unable to perform explicit MI could use implicit MI. Patients can easily understand a laterality judgement task than a task involving movement imagination which is often abstract. Unlike in the case of MI therapists can easily tell when the patients are correctly performing a judgement task.

Acknowledgement

This work is supported by the Engineering and Physical Sciences Research Council (EPSRC) Ph.D. grant (EP/P505534/1). The authors are grateful to Professor Frank Pollick for proofreading the paper.

References

Alivisatos, B., Petrides, M., 1996. Functional activation of the human brain during mental rotation. Neuropsychologia 35 (2), 111–118.
Bonda, E., Petrides, M., Frey, S., Evans, A., 1995. Neural correlates of mental transformations of the body-in-space. Proc. Natl. Acad. Sci. U. S. A. 92 (24), 11180–11184.
Bowering, K.J., O'Connell, N.E., Tabor, A., Catley, M.J., Leake, H.B., Moseley, G.L., Stanton, T.R., 2013. The effects of graded motor imagery and its components on chronic pain: a systematic review and meta-analysis. J. Pain 14 (1), 3–13.
Brett, M., Johnsrude, I.S., Owen, A.M., 2002. The problem of functional localization in the human brain. Nat. Rev. Neurosci. 3 (3), 243–249.
Cavanna, A.E., Trimble, M.R., 2006. The precuneus: a review of its functional anatomy and behavioural correlates. Brain 129 (3), 564–583.
Chen, X., Bin, G., Daly, I., Gao, X., 2013. Event-related desynchronization (ERD) in the alpha band during a hand mental rotation task. Neurosci. Lett. 541, 238–242.
Cohen, M.S., Kosslyn, S.M., Breiter, H.C., DiGirolamo, G.J., Thompson, W.L., Anderson, A., Bookheimer, S., Rosen, B.R., Belliveau, J., 1996. Changes in cortical activity during mental rotation a mapping study using functional MRI. Brain 119 (1), 89–100.
Comon, P., 1994. Independent component analysis, a new concept? Signal Process. 36 (3), 287–314.
Cooper, L.A., Shepard, R.N., 1975. Mental transformations in the identification of left and right hands. J. Exp. Psychol. Hum. Percept. Perform. 104 (1), 48–56.
Cramer, S.C., Orr, E.L., Cohen, M.J., Lacourse, M.G., 2007. Effects of motor imagery training after chronic, complete spinal cord injury. Exp. Brain Res. 177 (2), 233–242.
Crone, N.E., Miglioretti, D.L., Gordon, B., Sieracki, J.M., Wilson, M.T., Uematsu, S., Lesser, R.P., 1998. Functional mapping of human sensorimotor cortex with electrocorticographic spectral analysis. I. Alpha and beta event-related desynchronization. Brain 121 (12), 2271–2299.
Decety, J., Perani, D., Jeannerod, M., Bettinardi, V., Tadary, B., Woods, R., Mazziotta, J. C., Fazio, F., 1994. Mapping motor representations with positron emission tomography. Nature 371 (6498), 600–602.
Delorme, A., Makeig, S., 2004. EEGLAB: an open source toolbox for analysis of single-trial EEG dynamics including independent component analysis. J. Neurosci. Methods 134 (1), 9–21.
Dierks, T., Jelic, V., Pascual-Marqui, R.D., Wahlund, L.-O., Julin, P., Linden, D.E., Maurer, K., Winblad, B., Nordberg, A., 2000. Spatial pattern of cerebral glucose metabolism (PET) correlates with localization of intracerebral EEG-generators in Alzheimer's disease. Clin. Neurophysiol. 111 (10), 1817–1824.
Dijkerman, H.C., Ietswaart, M., Johnston, M., MacWalter, R.S., 2004. Does motor imagery training improve hand function in chronic stroke patients? A pilot study. Clin. Rehabil. 18 (5), 538–549.
Driskell, J.E., Copper, C., Moran, A., 1994. Does mental practice enhance performance? J. Appl. Psychol. 79 (4), 481–491.
Dyson, M., Sepulveda, F., Gan, J., 2010. Localisation of cognitive tasks used in EEG-based BCIs. Clin. Neurophysiol. 121 (9), 1481–1493.

Enzinger, C., Ropele, S., Fazekas, F., Loitfelder, M., Gorani, F., Seifert, T., Reiter, G., Neuper, C., Pfurtscheller, G., Müller-Putz, G., 2008. Brain motor system function in a patient with complete spinal cord injury following extensive brain-computer interface training. Exp. Brain Res. 190 (2), 215–223.
Epstein, R., Kanwisher, N., 1998. A cortical representation of the local visual environment. Nature 392 (6676), 598–601.
Fink, G.R., Frackowiak, R.S.J., Pietrzyk, U., Passingham, R.E., 1997. Multiple non-primary motor areas in the human cortex. J. Neurophysiol. 77 (4), 2164–2174.
Fletcher, P., Frith, C., Baker, S., Shallice, T., Frackowiak, R., Dolan, R., 1995. The mind's eye–precuneus activation in memory-related imagery. NeuroImage 2 (3), 195–200.
Gill, H.S., O'Boyle, M.W., Hathaway, J., 1998. Cortical distribution of EEG activity for component processes during mental rotation. Cortex 34 (5), 707–718.
Gogos, A., Gavrilescu, M., Davison, S., Searle, K., Adams, J., Rossell, S.L., Bell, R., Davis, S.R., Egan, G.F., 2010. Greater superior than inferior parietal lobule activation with increasing rotation angle during mental rotation: an fMRI study. Neuropsychologia 48 (2), 529–535.
Grangeon, M., Revol, P., Guillot, A., Rode, G., Collet, C., 2012. Could motor imagery be effective in upper limb rehabilitation of individuals with spinal cord injury? A case study. Spinal Cord 50 (10), 766–771.
Greenblatt, R.E., Ossadtchi, A., Pflieger, M.E., 2005. Local linear estimators for the bioelectromagnetic inverse problem. IEEE Trans. Signal Process. 53 (9), 3403–3412.
Hoffmann, S., Falkenstein, M., 2008. The correction of eye blink artefacts in the EEG: a comparison of two prominent methods. PLoS One 3 (8), e3004–e3004.
Holm, S., 1979. A simple sequentially rejective multiple test procedure. Scand. J. Stat. 6 (2), 65–70.
Hyvärinen, A., Oja, E., 2000. Independent component analysis: algorithms and applications. Neural Netw. 13 (4), 411–430.
Ionta, S., Fourkas, A.D., Fiorio, M., Aglioti, S.M., 2007. The influence of hands posture on mental rotation of hands and feet. Exp. Brain Res. 183 (1), 1–7.
Iriarte, J., Urrestarazu, E., Valencia, M., Alegre, M., Malanda, A., Viteri, C., Artieda, J., 2003. Independent component analysis as a tool to eliminate artifacts in EEG: a quantitative study. J. Clinical Neurophysiol. 20 (4), 249–257.
Jeannerod, M., 2006. Motor Cognition: What Actions Tell the Self, vol. 42. Oxford University Press, Oxford.
Jordan, K., Heinze, H., Lutz, K., Kanowski, M., Jäncke, L., 2001. Cortical activations during the mental rotation of different visual objects. Neuroimage 13 (1), 143–152.
Kanwisher, N., McDermott, J., Chun, M.M., 1997. The fusiform face area: a module in human extrastriate cortex specialized for face perception. J. Neurosci. 17 (11), 4302–4311.
Kosslyn, S.M., Alpert, N.M., Thompson, W.L., Maljkovic, V., Weise, S.B., Chabris, C.F., Hamilton, S.E., Rauch, S.L., Buonanno, F.S., 1993. Visual mental imagery activates topographically organized visual cortex: PET investigations. J. Cognit. Neurosci. 5 (3), 263–287.
Leech, R., Braga, R., Sharp, D.J., 2012. Echoes of the brain within the posterior cingulate cortex. J. Neurosci. 32 (1), 215–222.
Lotze, M., Halsband, U., 2006. Motor imagery. J. Physiol. Paris 99 (4), 386–395.
Makeig, S., 1993. Auditory event-related dynamics of the EEG spectrum and effects of exposure to tones. Electroencephalogr. Clin. Neurophysiol. 86 (4), 283–293.
Michel, C.M., Kaufman, L., Williamson, S.J., 1994. Duration of eeg and meg α suppression increases with angle in a mental rotation task. J. Cognit. Neurosci. 6 (2), 139–150.
Moseley, G.L., Butler, D.S., Beames, T.B., Giles, T.J., 2012. The Graded Motor Imagery Handbook. Noigroup Publications, Adelaide, Australia.
Mulert, C., Jäger, L., Schmitt, R., Bussfeld, P., Pogarell, O., Möller, H.-J., Juckel, G., Hegerl, U., 2004. Integration of fMRI and simultaneous EEG: towards a comprehensive understanding of localization and time-course of brain activity in target detection. Neuroimage 22 (1), 83–94.
Neuper, C., Pfurtscheller, G., 2001. Event-related dynamics of cortical rhythms: frequency-specific features and functional correlates. Int. J. Psychophysiol. 43 (1), 41–58.
Neuper, C., Wörtz, M., Pfurtscheller, G., 2006. ERD/ERS patterns reflecting sensorimotor activation and deactivation. In: Neuper, C., Klimesch, W. (Eds.), Event-related Dynamics of Brain Oscillations. Progress in Brain Research, vol. 159. Elsevier, Amsterdam, Netherlands, pp. 211–222.
Nichols, T.E., Holmes, A.P., 2002. Nonparametric permutation tests for functional neuroimaging: a primer with examples. Hum. Brain Mapp. 15 (1), 1–25.
Oldfield, R.C., 1971. The assessment and analysis of handedness: the Edinburgh inventory. Neuropsychologia 9 (1), 97–113.
Parsons, L.M., 1987a. Imagined spatial transformations of one's hands and feet. Cognit. Psychol. 19 (2), 178–241.
Parsons, L.M., 1987b. Imagined spatial transformation of one's body. J. Exp. Psychol. General 116 (2), 172.
Parsons, L.M., 1994. Temporal and kinematic properties of motor behavior reflected in mentally simulated action. J. Exp. Psychol. Hum. Percept. Perform. 20 (4), 709.
Parsons, L.M., 2001. Integrating cognitive psychology, neurology and neuroimaging. Acta psychol. 107 (1), 155–181.
Parsons, L.M., Fox, P.T., Downs, J.H., Glass, T., Hirsch, T.B., Martin, C.C., Jerabek, P.A., Lancaster, J.L., 1995. Use of implicit motor imagery for visual shape discrimination as revealed by PET. Nature 375 (6526), 54–58.
Pascual-Marqui, R., 2002. Standardized low-resolution brain electromagnetic tomography (sLORETA): technical details. Methods and Findings in Experimental and Clinical Pharmacology 24 (Suppl. D), 5–12.
Pascual-Marqui, R.D., 2007. Discrete, 3D distributed, linear imaging methods of electric neuronal activity. part 1: Exact, zero error localization. arXiv preprint arXiv:0710.3341.
Pascual-Marqui, R.D., Michel, C.M., Lehmann, D., 1994. Low resolution electromagnetic tomography: a new method for localizing electrical activity in the brain. Int. J. Psychophysiol. 18 (1), 49–65.
Pfurtscheller, G., 1992. Event-related synchronization (ERS): an electrophysiological correlate of cortical areas at rest. Electroencephalogr. Clin. Neurophysiol. 83 (1), 62–69.
Pfurtscheller, G., Aranibar, A., 1977. Event-related cortical desynchronization detected by power measurements of scalp EEG. Electroencephalogr. Clin. Neurophysiol. 42 (6), 817–826.
Pfurtscheller, G., Berghold, A., 1989. Patterns of cortical activation during planning of voluntary movement. Electroencephalogr. Clin. Neurophysiol. 72 (3), 250–258.
Pfurtscheller, G., Lopes da Silva, F.H., 1999. Event-related EEG/MEG synchronization and desynchronization: basic principles. Clin. Neurophysiol. 110 (11), 1842–1857.
Pfurtscheller, G., Leeb, R., Keinrath, C., Friedman, D., Neuper, C., Guger, C., Slater, M., 2006. Walking from thought. Brain Res. 1071 (1), 145–152.
Pfurtscheller, G., Scherer, R., Müller-Putz, G.R., Lopes da Silva, F.H., 2008. Short-lived brain state after cued motor imagery in naive subjects. Eur. J. Neurosci. 28 (7), 1419–1426.
Pizzagalli, D., Oakes, T., Fox, A., Chung, M., Larson, C., Abercrombie, H., Schaefer, S., Benca, R., Davidson, R., 2003. Functional but not structural subgenual prefrontal cortex abnormalities in melancholia. Mol. Psychiatry 9 (4), 393–405.
Riečansky`, I., Katina, S., 2010. Induced EEG alpha oscillations are related to mental rotation ability: the evidence for neural efficiency and serial processing. Neurosci. Lett. 482 (2), 133–136.
Sakata, H., Takaoka, Y., Kawarasaki, A., Shibutani, H., 1973. Somatosensory properties of neurons in the superior parietal cortex (area 5) of the rhesus monkey. Brain Res. 64, 85–102.
Scherer, R., rtsbci: a collection of methods and functions for real-time data acquisition, storage, signal processing and visualization based on matlab/simulink.
Schwarzlose, R.F., Baker, C.I., Kanwisher, N., 2005. Separate face and body selectivity on the fusiform gyrus. J. Neurosci. 25 (47), 11055–11059.
Sekihara, K., Sahani, M., Nagarajan, S.S., 2005. Localization bias and spatial resolution of adaptive and non-adaptive spatial filters for MEG source reconstruction. Neuroimage 25 (4), 1056–1067.
Shepard, R., Metzler, J., 1971. Mental rotation of three-dimensional objects. Science 171 (3972), 701–703.
Takeda, K., Shimoda, N., Sato, Y., Ogano, M., Kato, H., 2010. Reaction time differences between left- and right-handers during mental rotation of hand pictures. Laterality 15 (4), 415–425.
Talairach, J., Tournoux, P., 1988. Co-planar stereotaxic atlas of the human brain: 3-dimensional proportional system: an approach to cerebral imaging. Thieme.
Vingerhoets, G., de Lange, F.P., Vandemaele, P., Deblaere, K., Achten, E., 2002. Motor imagery in mental rotation: an fMRI study. Neuroimage 17 (3), 1623–1633.
Vitacco, D., Brandeis, D., Pascual-Marqui, R., Martin, E., 2002. Correspondence of event-related potential tomography and functional magnetic resonance imaging during language processing. Hum. Brain Mapp. 17 (1), 4–12.
Vuckovic, A., Osuagwu, B.A., 2013. Using a motor imagery questionnaire to estimate the performance of a brain-computer interface based on object oriented motor imagery. Clin. Neurophysiol. 124 (8), 1586–1595.
Walz, A.D., Usichenko, T., Moseley, G.L., Lotze, M., 2013. Graded motor imagery and the impact on pain processing in a case of CRPS. Clin. J. Pain 29 (3), 276–279.
Weiss, M.M., Wolbers, T., Peller, M., Witt, K., Marshall, L., Buchel, C., Siebner, H.R., 2009. Rotated alphanumeric characters do not automatically activate frontoparietal areas subserving mental rotation. NeuroImage 44 (3), 1063–1073.
Wexler, M., Kosslyn, S.M., Berthoz, A., 1998. Motor processes in mental rotation. Cognition 68 (1), 77–94.
Wolpaw, J.R., Birbaumer, N., McFarland, D.J., Pfurtscheller, G., Vaughan, T.M., 2002. Brain-computer interfaces for communication and control. Clin. Neurophysiol. 113 (6), 767–791.
Worrell, G.A., Lagerlund, T.D., Sharbrough, F.W., Brinkmann, B.H., Busacker, N.E., Cicora, K.M., O'Brien, T.J., 2000. Localization of the epileptic focus by low-resolution electromagnetic tomography in patients with a lesion demonstrated by MRI. Brain Topogr. 12 (4), 273–282.
Wraga, M., Thompson, W.L., Alpert, N.M., Kosslyn, S.M., 2003. Implicit transfer of motor strategies in mental rotation. Brain Cognit. 52 (2), 135–143.
Young, R.K., 1993. Wavelet Theory and its Applications, vol. 189. Kluwer academic publishers, Massachusetts, USA.
Zacks, J.M., 2008. Neuroimaging studies of mental rotation: a meta-analysis and review. J.Cognit. Neurosci. 20 (1), 1–19.
Zumsteg, D., Wennberg, R.A., Treyer, V., Buck, A., Wieser, H.G., 2005. H215O or 13NH3 PET and electromagnetic tomography (LORETA) during partial status epilepticus. Neurology 65 (10), 1657–1660.